Structural Properties of the Ion-Dipole Model of Electrolyte Solutions in the Bulk and Near a Charged Hard Wall. Application of the Truncated Optimized Cluster Series

O. A. Pizio

Department of Chemistry, University of Utah, Salt Lake City, Utah 84112, USA

Z. B. Halytch

Lviv University, Lviv, 29000, USSR

Z. Naturforsch. **46a**, 8–18 (1991); received July 23, 1990

Dedicated to Dr. Karl Heinzinger on the occasion of his 60th birthday

An ion-dipole model of electrolyte solutions in the bulk case and near a charged or uncharged hard wall is considered. A method to derive the terms of optimized cluster expansions for the distribution functions of ions and dipoles which provides a set of approximations beyond the mean spherical approximation is given. The third cluster coefficient approximation is investigated.

1. Introduction

Enlarged computer facilities have provided the possibility to simulate ion-aqueous systems with a high degree of sophistication and to obtain very detailed information about the properties of electrolyte solutions [1–16]. Also water and aqueous electrolytes at interfaces have been MD simulated [7–10]. These computer experiments have stimulated theoretical investigations. Actually simulation and theory supplement each other, and comparisons of the results of the two methods have become possible [11].

The current theory of electrolyte solutions is based on ion-multipole models and has gained impressive profit by the application of the reference hypernetted chain (RHNC) integral equation [12–14]. The solvent molecules considered in this set of papers consist of hard spheres with embedded water-like dipole and quadrupole moments. Despite the simplicity of the model if compared with the one commonly used for the simulations the resulting structural and thermodynamic properties are quite correct. Recently the RHNC treatment has been applied to solvents in the vicinity of a hard wall [15–17]. For completeness we mention that ionic solutions have also been treated within rigid site-site and flexible models [18, 19] which are not restricted to the multipole expansion and are more appropriate for intermediate interparticle distances. But still, simpler models remain attractive and the mean spherical approximation (MSA) integral equation, which possesses analytic solutions for the ion-dipole mixture retains its importance.

The MSA is linear in the strength of the interactions, and so its application is quite limited. One needs a nonlinear theory which incorporates many-particle correlations. This is important for instance for the description of the electric field dependent structure of electrolyte solutions near a surface. In this case the saturation effects at the increasing field have to be described by the theory.

In our opinion, a qualitatively correct treatment which satisfies all the demands remarked previously is given by the optimized cluster theory (OCT). We have found that optimized cluster expansions can describe quite satisfactorily the structural properties of molten ionic systems [20, 21], of electrolyte solutions [22] and their properties near a charged or uncharged hard wall [23, 24].

In this paper we study some of the exponential approximations for the distribution functions of electrolyte solutions. The bulk model and the corresponding one for contact with a charged hard wall will be considered. In the bulk model, the pair distribution functions provide detailed information on the radial and angular correlations between the ions and solvent molecules. The corresponding one-particle distribution functions for the ion-dipole mixture near a charged or uncharged wall yield then the density profiles, the charge and polarization density profiles, and informa-

Reprint requests to Dr. O. A. Pizio, Lviv Department of the Institute for Theoretical Physics, Ukrainian Academy of Science, Lviv, 290005, USSR.

0932-0784 / 91 / 0100-0008 $ 01.30/0. – Please order a reprint rather than making your own copy.

tion concerning the angular correlations of the solvent molecules in the interfacial layer.

The results presented here will be discussed in context of the more realistic simulations and RHNC theory. We analyze the optimized cluster expansions as a perturbation theory and show that allowance for the cluster coefficients in the OCT is of crucial importance to provide an adequate description of structural properties.

2. Ion-dipole Model of Electrolyte Solutions. Exponential Approximations for the Pair Distribution Functions within OCT

The simplest, nonprimitive model of electrolyte solutions is the ion-dipole hard sphere mixture. Unlike the primitive models, the solution consists of two subsystems: the solute consists of hard spheres carrying the charges q_+ and q_- ($q_+ = |-q_-| = q$), and the solvent consists of hard spheres of density ϱ_s, possessing the dipole moments μ_s. All the spheres have the same diameter ($\sigma_+ = \sigma_- = \sigma_s = \sigma$). The system is electroneutral in total, $\varrho_+ = \varrho_i/2 = \varrho_-$, where ϱ_i denotes the density of the ions. The state of the model is given by a set of dimensionless reduced parameters, namely the packing fraction $\eta = \pi(\varrho_i + \varrho_s)\sigma^3/6$, the ion concentration $c_i = \varrho_i/(\varrho_i + \varrho_s)$, and the reverse ion and dipole "temperatures" $q_i^* = q^2/kT\sigma$, $\mu_s^* = \mu_s^2/kT\sigma^3$.

Obviously, there are various possibilities to refine the model. One can allow for higher multipoles and different sizes of the particles or other interactions. We are presently engaged in these problems.

In order to derive the optimized cluster expansions (OCE) one can use an integral equation for the pair distribution functions (p.d.fs) which has been represented already for the bulk model and the one near a wall [23–25] in the following form

$$g_{xy}(12) = g_{xy}^{(0)}(r_{12}) \exp\{G_{xy}(12) + \delta h_{xy}(12) - \delta c_{xy}(12) + \Delta E_{xy}(12)\} \quad (1)$$

where

$$\delta h_{xy}(12) - \delta c_{xy}(12) = \delta c_{xt}(13) \bullet\!\!\wedge\!\!\circ H_{ty}(32) + h_{xt}(13) \bullet\!\!\wedge\!\!\circ \delta c_{ty}(32) + h_{xt}(13) \; \delta c_{tn}(34) \; H_{ny}(42). \quad (2)$$

The black circle in Eq. (2), i.e. the field vertex, denotes the sum over the species and integration over the coordinates, both translational and rotational ($\bullet \to \sum_l \varrho_l \int dr_3 \, d\Omega_3$). The hard-sphere reference fluid has been applied in (1), so $g_{xy}^{(0)}(12) = g_{xy}^{(0)}(r_{12})$, which depends only on the packing fraction as a parameter. Other notations in (1) and (2) are: $G_{xy}(12)$ is the renormalized or so called screened potential of interparticle interaction [26],

$$H_{xy}(12) = H_{xy}^{(MSA)}(12) = g_{xy}^{(0)}(r_{12}) - 1 + G_{xy}(12) \quad (3)$$

is the pair correlation function within the mean spherical approximation [27],

$$\delta h_{xy}(12) = g_{xy}(12) - 1 - H_{xy}(12) = h_{xy}(12) - H_{xy}(12), \quad (4)$$

where $h_{xy}(12)$ is the desired form of the pair correlation function, $\Delta E_{xy}(12)$ is the difference between the bridge diagrams contribution for the system under consideration and the one for the reference fluid. One can easily rewrite (1) in the form

$$\delta c_{xy}(12) = g_{xy}(12) - g_{xy}^{(0)}(r_{12}) - \ln[g_{xy}(12)/g_{xy}^{(0)}(r_{12})] + \Delta E_{xy}(12). \quad (5)$$

We have to note that the bridge diagrams are constructed on the $h_{xy}(12)$ lines and their contribution will depend on the choice of the approximate form of $h_{xy}(12)$. The calculation of even the simplest bridge diagrams is a difficult task, therefore the theories developed up to date either neglect this term (HNC) or allow for it in a simplified manner [19]. We shall neglect the term $\Delta E_{xy}(12)$ in the following derivation.

Now, the construction of the OCE can be given from the initial equations (1), (2), and (5) as follows. One can start from the EXP 2 approximation in (1)

$$h_{xy}^{(EXP2)}(12) = g_{xy}^{(0)}(r_{12}) \exp[G_{xy}(12)] - 1, \quad (6)$$

which determines then the function $\delta c_{xy}(12)$ according to (5):

$$\delta c_{xy}(12) = g_{xy}^{(0)}(r_{12})[e^{G_{xy}(12)} - 1] - G_{xy}(12) = h_{xy}^{(EXP2)}(12) - H_{xy}(12). \quad (7)$$

Then, substituting the functions (6) and (7) into (1), with accuracy of diagrams with only one field vertex, one obtains the EXP 3 approximation

$$g_{xy}^{(EXP3)}(12) = g_{xy}^{(0)}(r_{12}) \exp\left\{G_{xy}(12) + h_{xt}^{(EXP2)}(13) \bullet\!\!\wedge\!\!\circ h_{ty}^{(EXP2)}(32) - H_{xt}(13) \bullet\!\!\wedge\!\!\circ H_{ty}(32)\right\} = g_{xy}^{(0)}(r_{12}) \exp\{G_{xy}(12) + G_{xy}^{(3)}(12)\}, \quad (8)$$

where the set of two diagrams in the exponent in (8) is called the third cluster coefficient. Let us discuss this approximation with a few words.

It has to be noted that in the EXP2 the allowance for many-particle correlations, similarly to the MSA, is given through the renormalized interaction $G_{xy}(12)$ which contains the effect of the medium. Contrarily to the MSA, given by (3), which is linear in the renormalized potential, the EXP2 introduces a strong nonlinearity in the strength of interaction. It is known that the MSA leads to an unphysical behaviour of $g_{ii}(r)$ at increasing strength of the interaction. On the other hand, this theory satisfies the exact sum rules for the pair distribution functions [27], which are the analogues of the Stillinger-Lovett electroneutrality conditions for pure ionic systems (see, for instance [28]).

The set of exponential approximations produces the p.d.fs $g_{ii}(r)$ which are positively defined everywhere, contrary to the MSA. However, the truncated versions of the OCE do not satisfy exactly the aforementioned sum rules. We have already investigated the truncated OCE for pure ionic systems. It was shown that the violation of local electroneutrality at increasing strength of interactions can be decreased only if one applies EXP4 and higher order approximations. We have not investigated yet this problem for the ion-dipole model, and therefore terms of the OCE higher than EXP2 will be discussed only at comparatively weak interparticle interactions to illustrate the OCE as a perturbation theory.

The EXP3 form contains explicitly the correlations within the three-particle "cluster" besides the effect of the medium by means of $G_{xy}(12)$. It is clear that this form, similarly to the EXP2, will be more or less appropriate depending on the thermodynamic state of the model.

If one allows for the term with two field vertices in (2), then the p.d.fs contain chain correlations with one and two field vertices. As previously, the diagrams are constructed on the $h_{xy}^{(\mathrm{EXP2})}(12)$ and $H_{xy}(12)$ lines. This form with $\delta c_{xy}(12)$ determined by EXP2 can be applied as the input for the iterative procedure, which finally has to produce the RHNC result. The method presented here differs from usual HNC by the application of non-point optimized renormalized potentials and by the separation of the reference fluid contribution. The convergence of the numerical iterative procedure has to be investigated separately, especially if one reminds that the MSA applied in it introduces inaccuracies in the treatment of size difference effects.

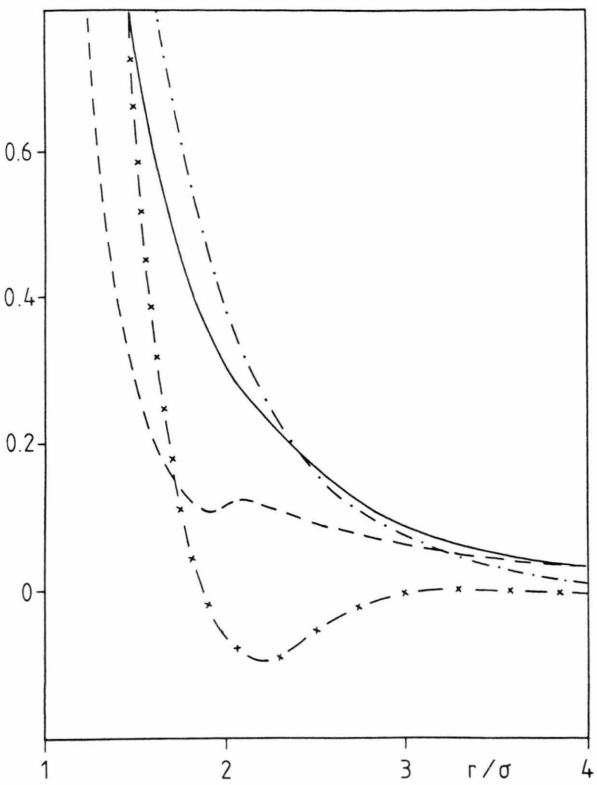

Fig. 1. Renormalized potentials of ion-ion interaction for $c_i=0.0625$; $q_i^*=3$, $\mu_s^*=0.5$ (full line), $q_i^*=3$, $\mu_s^*=2$ (dashed line), $q_i^*=6$, $\mu_s^*=0.5$ (dash dot). $c_i=0.222$; $q_i^*=8$, $\mu_s^*=0.5$ ($-\times-\times-$). In Figs. 1–7 $\eta=0.31415$.

We have to note that the iterative procedure is not the unique path to determine the p.d.fs. It can happen that the direct solution of (2) is necessary for some cases. Previously, the traditional method of classification of the OCE terms by the number of field vertices has been used in the studies of electrolyte solutions [26].

In order to illustrate the application of optimized cluster series we shall start from general remarks. The p.d.fs of the hard-sphere reference fluid will be calculated within the Percus-Yevick approximation, which is qualitatively correct at liquid densities. Independently of the path used to sum up the cluster series, the key functions for OCEs are the renormalized potentials. They are calculated from the MSA analytic solution for the corresponding model [27]. One has to note that the angular dependence of renormalized potentials within the MSA is similar to the one for the initial interactions. Two different representations of the angular dependent functions are necessary either for the calculation of renormalized potentials or for the inte-

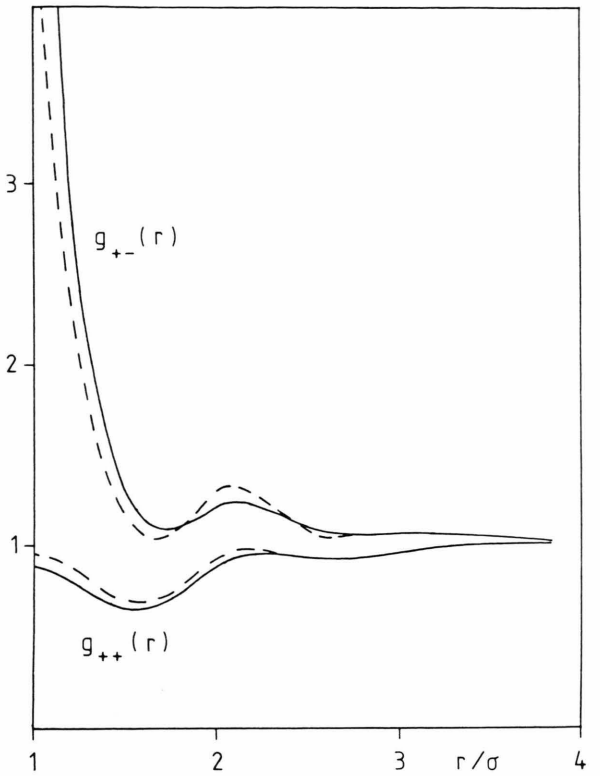

Fig. 2. Ion-ion pair distribution functions (p.d.fs) for $c_i = 0.0625$, $q_i^* = 3$, $\mu_s^* = 0.5$. EXP 2 (full line), EXP 3 (dashed line).

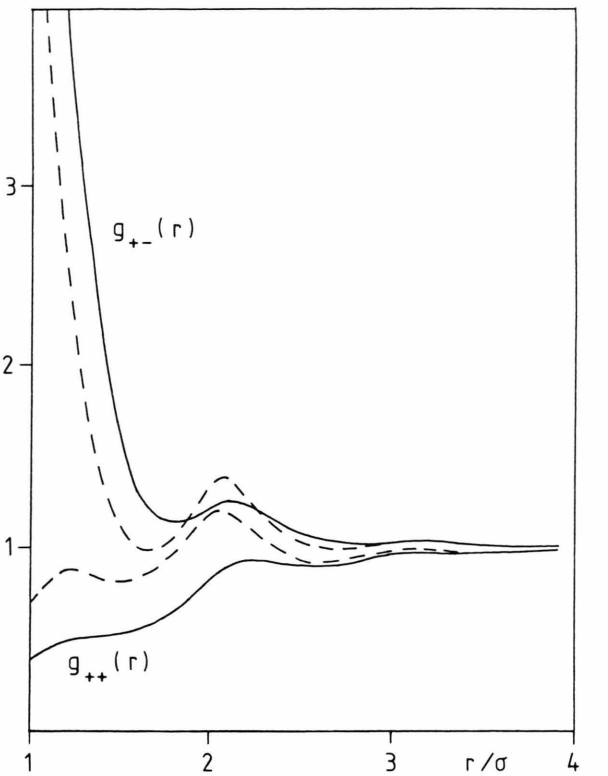

Fig. 3. Ion-ion p.d.fs for $c_i = 0.0625$, $q_i^* = 6$, $\mu_s^* = 0.5$. EXP 2 (full line), EXP 3 (dashed line).

gration over rotational degrees of freedom in the calculation of the cluster series. One has to apply both the orientational expansion in the intermolecular frame

$$f_{xy}(12) = \sum_{mn,\,\mu\nu\chi} f^{mn}_{xy,\,\mu\nu\chi}(r_{12})\, \bar{\Phi}^{mn}_{\mu\nu,\,\chi}(\Omega_1, \Omega_2) \qquad (9)$$

and the orientation-invariant expansion in the laboratory frame

$$f_{xy}(12) = \sum_{\substack{mnl \\ \mu\nu}} f^{mnl}_{xy,\,\mu\nu}(r_{12})\, \tilde{\Phi}^{mnl}_{\mu\nu}(\Omega_1, \Omega_2, \Omega_{\mathbf{r}_{12}}), \qquad (10)$$

where

$$\tilde{\Phi}^{mnl}_{\mu\nu}(\Omega_1, \Omega_2, \Omega_{\mathbf{r}_{12}}) = [(2m+1)(2n+1)]^{1/2} \cdot \sum_{\mu'\nu'\lambda'} \begin{pmatrix} m & n & l \\ \mu' & \nu' & \lambda' \end{pmatrix} \mathscr{D}^{m}_{\mu\mu'}(\Omega_1)\, \mathscr{D}^{n}_{\nu\nu'}(\Omega_2)\, \mathscr{D}^{l}_{0\lambda'}(\Omega_{\mathbf{r}_{12}}) \qquad (11)$$

are the rotational invariants

$$\bar{\Phi}^{mn}_{\mu\nu\chi}(\Omega_1, \Omega_2) = [(2m+1)(2n+1)]^{1/2}\, \mathscr{D}^{m}_{\mu\chi}(\Omega_1)\, \mathscr{D}^{n}_{\nu-\chi}(\Omega_2) \qquad (12)$$

and $\mathscr{D}^{m}_{\mu\mu'}(\Omega_i)$ denote the generalized spherical functions and $\begin{pmatrix} m & n & l \\ \mu & \nu & \lambda \end{pmatrix}$ are $3j$-symbols. The method to calculate the coefficients of the orientation-invariant expansion for the ion-dipole mixture ($\mu = \nu = 0$) has been presented in [27].

Let us restrict ourselves in this study by the EXP 3 approximation. The p.d.fs are also expanded into the orientation-invariant series

$$g_{is}(r, \Omega_s) = g_{is}^{(000)}(r) + g_{is}^{(101)}(r)\, \tilde{\Phi}^{101}(0, \Omega_s, \Omega_r) + \ldots \qquad (13)$$

$$g_{st}(r, \Omega_s, \Omega_t) = g_{st}^{(000)}(r) + g_{st}^{(110)}(r)\, \tilde{\Phi}^{110}(\Omega_s, \Omega_t, \Omega_r) + g_{st}^{(112)}(r)\, \tilde{\Phi}^{112}(\Omega_s, \Omega_t, \Omega_r), \qquad (14)$$

and the ion-ion functions are given directly by (8). A set of results for the ion-dipole mixture in the bulk is presented in Figures 1–7. The ion-ion renormalized potentials are shown in the Figure 1. At low strength of both ion-ion and dipole-dipole interactions the behaviour of $G_{ij}(r)$ is similar to the case of Debye screening. With increasing q_i^* the correlation length decreases and then the curve changes its shape to oscillatory, which describes the arising ionic short-range ordering in the system. With increasing μ_s^* at low q_i^* the polar solvent influences the ionic screening.

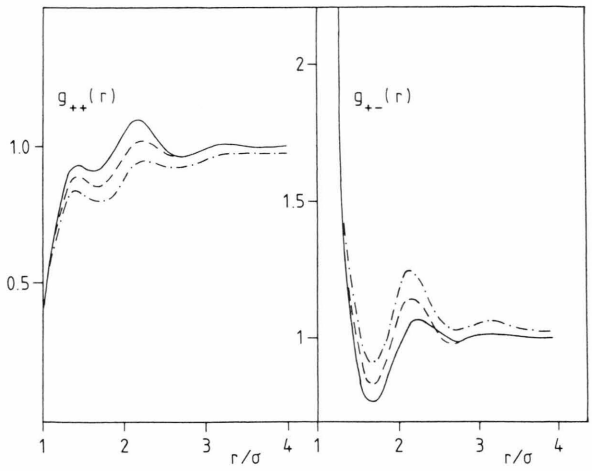

Fig. 4. Concentration dependence of the ion-ion p.d.fs within EXP2 approximation for $q_i^* = 13.6$, $\mu_s^* = 3.15$. $c_i = 0.5$ (full line), $c_i = 0.222$ (dashed line), $c_i = 0.0625$ (dash dot).

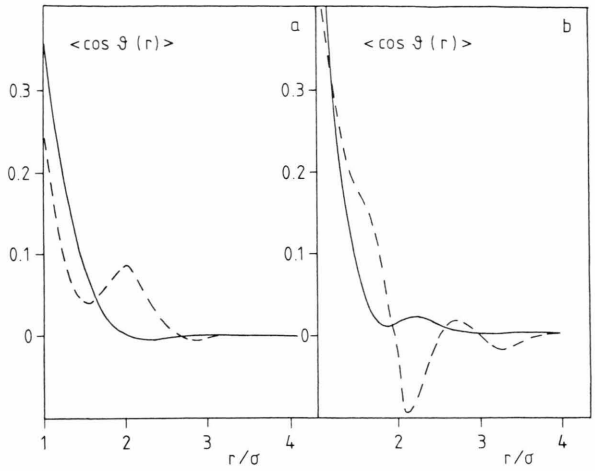

Fig. 6. $\langle \cos \vartheta(r) \rangle$ dependence on the reverse dipole "temperature". The parameters are as in Figure 5. EXP2 (full line), EXP3 (dashed line).

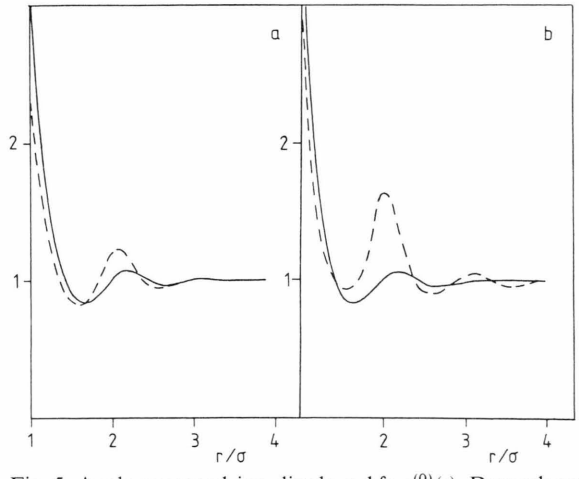

Fig. 5. Angle averaged ion-dipole p.d.fs $g_{is}^{(0)}(r)$. Dependence on reverse dipole "temperature" (a: $\mu_s^* = 0.5$, b: $\mu_s^* = 2.0$), $c_i = 0.222$, $q_i^* = 6$; EXP2 (full line), EXP3 (dashed line).

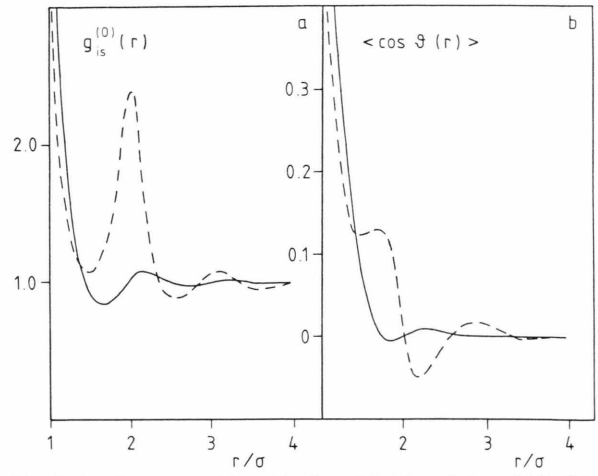

Fig. 7. Angle averaged ion-dipole p.d.fs (a) and $\langle \cos \vartheta(r) \rangle$ (b) for $c_i = 0.222$, $q_i^* = 12$, $\mu_s^* = 2$; EXP2 (full line), EXP3 (dashed line).

The Debye-like picture is modified by the solvation effects in this case. The ion-ion distribution functions are presented in the following figures. Everywhere the packing fraction corresponds to the dense fluid $\eta = 0.31415$. At low values of q_i^* and μ_s^* ($c_i = 0.0625$) both exponential approximations give similar results for $g_{++}(r)$ and $g_{+-}(r)$ ($g_{++}(r) = g_{--}(r)$ due to the symmetry of the model considered). In this case the contribution of the third cluster coefficient is really the perturbation of the qualitatively correct picture given by the EXP2 (Figure 2). With increasing dipole strength the contact value $g_{++}(\sigma+)$ becomes larger than unity, however, $g_{++}(\sigma+) \ll g_{+-}(\sigma+)$. With increasing ion strength parameter the difference between the EXP2 and EXP3 results increases for the function $g_{++}(r)$, while $g_{+-}(r)$ is quite similar within both approximations (Figure 3). We have to conclude than that in order to provide the qualitatively correct picture of both ion-ion p.d.fs it is necessary to apply either different levels of truncation of the OCE for $g_{+-}(r)$ and $g_{++}(r)$ or to apply an iterative procedure with an infinite number of steps in order to achieve the RHNC

results. The dependence of $g_{+-}(r)$ and $g_{++}(r)$ on the ion concentration is presented in the Figure 4. The shape of the curves changes smoothly, reflecting the transition from the Debye-like picture modulated by the solvation effects to the ionic ordering at very high ion concentrations. Actually, the predictions for $g_{ij}(r)$ dependent on c_i coincide with the ones obtained by more elaborated RHNC theory at larger q_i^* [15]. In fact, the ion-ion p.d.fs have to be discussed simultaneously with the ion-molecule distribution function, namely the ion-dipole function for the model considered. In case of the ion-dipole mixture the ion-dipole p.d.f. can be expanded as follows [22]:

$$g_{si}(r,\vartheta)=g_{si}^{(0)}(r)\exp\left\{\sqrt{3}\,G_{si}^{10}(r)\cos\vartheta + \sum_{k\geqq 0}\sqrt{2k+1}\,G_{si}^{(3)k0}(r)\,\mathscr{P}_k(\cos\vartheta)\right\}$$
$$=\sum_{n\geqq 0}\tilde{g}_{si}^{(n)}(r)\,\mathscr{P}_n(\cos\vartheta), \tag{15}$$

where ϑ is the angle between the dipole moment direction and the ion-dipole axis, and $\mathscr{P}_n(\cos\vartheta)$ denotes the Legendre polynomials. Then, the contribution independent of the orientations is

$$\tilde{g}_{si}^{(0)}(r)\cong\tfrac{1}{2}\,g_2^{(0)}(r) \cdot\exp\left[G_{si}^{(3)00}(r)\right]\cdot\frac{\operatorname{sh}\left[\sqrt{3}\,G_{si}^{10}(r)+\sqrt{3}\,G_{si}^{(3)10}(r)\right]}{\sqrt{3}\left[G_{si}^{10}(r)+G_{si}^{(3)10}(r)\right]}. \tag{16}$$

It describes the effects of density ordering of dipoles with respect to the chosen ion and consists of the pure hard-sphere contribution and the one from electrostatic interactions by means of the renormalized potential and the cluster terms.

Besides that, $g_{si}(r,\vartheta)$ provides the possibility to analyze the angular distribution of dipole moment dependent on the distance between ion and dipole

$$\langle\cos\vartheta\rangle=\int\cos\vartheta\,g_{si}(r,\vartheta)\sin\vartheta\,d\vartheta\Big/\int g_{si}(r,\vartheta)\sin\vartheta\,d\vartheta$$
$$=\tilde{g}_{si}^{(1)}(r)/\tilde{g}_{si}^{(0)}(r), \tag{17}$$

which has already been studied for the ion-dipole-quadrupole model by means of RHNC [13, 14]. In order to investigate the angular correlations in the first hydration shell it is helpful to consider the function

$$\bar{g}_{si}(\cos\vartheta)=\int_0^{r_{si}^*} g_{si}(r,\vartheta)\,dr, \tag{18}$$

where r_{si}^* is chosen as a distance providing the hydration number of ions [3], which corresponds usually to the first minimum of the ion-dipole p.d.f. One can construct also the mean square fluctuation

$$\langle\cos^2\vartheta(r)\rangle-\langle\cos\vartheta(r)\rangle^2$$

which reflects qualitatively the reorientation of dipolar molecules dependent on the distance.

The angle averaged ion-dipole distribution function is presented in Figure 5. As previously, the difference between the EXP2 and EXP3 results increases with increasing values of the parameters q_i^* and μ_s^*. While the EXP2 produces a function very similar to the hard-sphere d.f., the EXP3 provides a higher second peak and more pronounced oscillations. The analysis of RHNC results [15] support us in claiming the EXP2 data to be qualitatively more correct, and therefore one has to be careful at the truncation of the OCE at any chosen step. The oscillations of the expansion coefficients $\tilde{g}_{si}^{(0)}(r)$, $\tilde{g}_{si}^{(1)}(r)$ result in the oscillatory behaviour of $\langle\cos\vartheta(r)\rangle$ (Fig. 6) which has been discussed in [12]. However the oscillations of $\langle\cos\vartheta(r)\rangle$ are much weaker within the EXP2 than the EXP3 due to the low values of q_i^* and μ_s^* and much weaker solvation effects already mentioned for the model of equal sizes [15] than for a more realistic model [12] with nonequal sizes of cations, anions and molecules.

Now, from the set data presented here one can make the following conclusions. The first point necessary to note is that we cannot estimate the quality of the results because simulations with different sets of parameters for the ion-dipole mixture are yet unavailable, except [11, 29]. We can state, however, that EXP2 in general provides a qualitatively correct and physically transparent picture of the structural properties (see also [22]). At high strengths of ion-ion and dipole-dipole interactions the EXP2 data become poorer. Here, we have attempted to include the first cluster term besides the effects of screening. It appears then that at high values of q_i^* and μ_s^* the difference between both sets of data is considerable, contrary to low values of q_i^*, μ_s^*. In this case the contribution of the third cluster coefficient is a perturbation to the renormalized potential. However, one can claim that either EXP2 or EXP3 provides a shape of the ion-ion and ion-dipole p.d.fs which has much in common with the one obtained by means of the much more elaborated RHNC theory. We can state now that EXP3 truncation of the OCE is insufficient if one wants to use the theory at normal temperatures and water-like dipole moments. We hope that the inclusion of the correlations within higher order clusters, i.e. EXP4 or It1 [20, 24], will provide a qualitatively correct picture

of ionic solvation. What makes us sure at this point is the similarity of the method applied here to the one with point particles' screening and the analysis of the result of the latter [30]. Actually, the quality of results obtained by the OCE method, if the cluster series would be calculated by means of the iterative procedure will depend on the choice of the initial form for $g_{ij}(r)$ and $g_{is}(r, \vartheta)$. Even from the EXP 3 calculations one can see that the EXP 2 form is insufficient to be used as initial one for $g_{+-}(r)$ at high q_i^* and μ_s^*. Therefore, the linearized version

$$g_{+-}(r) = g_{++}^{(0)}(r)\,[1 + G_{+-}(r)] \tag{19}$$

can be used as an alternative for the iterative treatment. Besides that, it would be very important while going further to the more realistic models, to allow for the softness of realistic repulsion in the reference fluid description and for the construction of soft-core screened potentials in order to reproduce correctly the heights of at least the first peaks of p.d.fs. The dipole-dipole p.d.f. and higher order terms for the $g_{ij}(r)$ and $g_{is}(r, \vartheta)$ will be investigated in forthcoming papers.

3. Ion-dipole Model of Electrolyte Solution in Contact with an Uncharged or Charged Hard Wall

The methods which have been applied for electrolyte solutions in the bulk and which were enumerated in the introduction provide a basis which one can use to develop a theory of electric double layer models. This generalization becomes possible by applying the Henderson-Abraham-Barker [31] and Percus [32] procedure for a bulk many-sort model in the limits of infinite dilution for the "wall" particles and infinite increase of their size. In this case, as in most of other theoretical studies, the structure of the electrode is disregarded. However, the geometrical restrictions due to the presence of the either uncharged or charged hard wall are allowed for. It must be noted that, as for the bulk case, all the existing approximate theories become poorer with increasing intensity of interparticle and particle-wall interactions.

If the aforementioned procedure is applied for the ion-dipole mixture then the ion-wall distribution function $g_{iw}(z)$ and position-orientation dependent dipole profile $g_{sw}(z, \vartheta)$ become available. These functions provide a large set of properties including the charge and polarization density profiles, the orientational distribution of dipoles in the interface region, the potential profile and the potential drop. Also the differential capacity and adsorption isotherms can be calculated.

The ion-dipole mixture in contact with a charged or uncharged hard wall can be characterized by the same set of parameters as the bulk, and in addition by the reduced dimensionless field strength $E^* = (\sigma^3/kT)^{1/2}\,4\pi\tau$, where τ denotes the homogeneous charge density on the wall.

We shall not repeat the derivation of the OCE for the model near the wall as it has been presented already in [23, 24]. The particle wall distribution functions are given in the form

$$g_{xw}(z, \vartheta) = g_{xw}^{(0)}(z) \exp\,[G_{xw}(z, \vartheta) + \delta h_{xw}(z, \vartheta) - \delta c_{xw}(z, \vartheta) + \Delta E_{xw}(z, \vartheta)] \tag{20}$$

or

$$\delta c_{xw}(z, \vartheta) = g_{xw}(z, \vartheta) - g_{xw}^{(0)}(z, \vartheta) - \ln\,[g_{xw}(z, \vartheta)/g_{xw}^{(0)}(z)] + \Delta E_{xw}(z, \vartheta) \tag{21}$$

and

$$\delta h_{xw}(z, \vartheta) - \delta c_{xw}(z, \vartheta) \tag{22}$$

$$= \delta c_{xy}^{(B)} \; \overset{y}{\underset{x \quad w}{\wedge}} \; H_{yw} + h_{xy}^{(B)} \; \overset{y}{\underset{x \quad w}{\wedge}} \; \delta c_{yw} + h_{xy}^{(B)} \; \overset{\delta c_{yt}^{(B)}}{\underset{x \quad w}{\sqcap}} \; H_{tw},$$

where the following notations have been introduced: z is the distance of the particle x from the wall, ϑ is the dipole moment angle with respect to the surface normal, $g_{xw}^{(0)}(z)$ corresponds to the reference fluid of hard spheres near a hard wall. The set of renormalized potentials is obtained from the one-particle distribution functions of the MSA analytical solution [33] by the subtraction of the reference fluid contribution.

Similarly to the treatment of bulk ion-dipole model we have introduced in (20) the deviations of the correlation functions from the MSA solution

$$h_{xw}(z, \vartheta) = g_{xw}(z, \vartheta) - 1 = H_{xw}^{(MSA)}(z, \vartheta) + \delta h_{xw}(z, \vartheta), \tag{23}$$

$$c_{xw}(z, \vartheta) = C_{xw}^{(MSA)}(z, \vartheta) - \delta c_{xw}(z, \vartheta), \tag{24}$$

where $c_{xw}(z, \vartheta)$ is the particle-wall direct correlation function, and the MSA solution provides the following form for the correlation functions:

$$H_{xw}^{(MSA)}(z, \vartheta) = g_{xw}^{(0)}(z) - 1 + G_{xw}(z, \vartheta), \tag{25}$$

$$C_{xw}^{(MSA)}(z, \vartheta) = c_{xw}^{(0)}(z) - \frac{1}{kT}\,\Phi_{xw}(z, \vartheta) \tag{26}$$

and there $\Phi_{xw}(z, \vartheta)$ are the electrostatic particle-wall interactions

$$\begin{aligned} \Phi_{iw}(z) &= -eEz, \qquad z > \sigma/2; \\ \Phi_{sw}(z, \vartheta) &= -\mu_s E \cos\vartheta, \quad z > \sigma/2, \end{aligned} \tag{27}$$

The superscript (B) in (20)–(22) denotes that these functions correspond to the bulk electrolyte model.

In order to analyse the cluster terms in (20) one can start from the EXP 2 approximation for the particle-wall distribution functions

$$g_{xw}^{(EXP2)}(z, \vartheta) = g_{xw}^{(0)}(z) \exp[G_{xw}(z, \vartheta)], \tag{28}$$

which gives $\delta c_{xw}(z, \vartheta)$ in the form

$$\begin{aligned} \delta c_{xw}(z, \vartheta) &= g_{xw}^{(0)}(z) \{\exp[G_{xw}(z, \vartheta)] - 1\} - G_{xw}(z, \vartheta) \\ &= h_{xw}^{(EXP2)}(z, \vartheta) - H_{xw}^{(MSA)}(z, \vartheta). \end{aligned} \tag{29}$$

The EXP 3 approximation is determined then as follows:

$$g_{xw}^{(EXP3)}(z, \vartheta) = g_{xw}^{(EXP2)}(z, \vartheta) \tag{30}$$

$$\cdot \exp\left\{\delta c_{xy}^{(B)} \bigwedge H_{yw}^{(MSA)} + h_{xy}^{(B)} \bigwedge h_{yw}^{(EXP2)} - h_{xy}^{(B)} \bigwedge H_{yw}^{(MSA)}\right\}.$$

We have to specify now the bulk correlation functions. If one chooses the EXP 2 form of $\delta c_{xy}^{(B)}$, then the particle-wall distribution function is

$$g_{xw}^{(EXP3)}(z, \vartheta) = g_{xw}^{(EXP2)}(z, \vartheta) \tag{31}$$

$$\cdot \exp\left\{h_{xy}^{(EXP2)} \bigwedge h_{yw}^{(EXP2)} - H_{xy}^{(MSA)} \bigwedge H_{yw}^{(MSA)}\right\},$$

which we shall call define as EXP 3 (E 2, E 2) approximation to emphasize that the EXP 2 choice has been applied for the bulk functions and particle-wall ones in the $G_{xw}^{(3)}(z, \vartheta)$. Equation (31) has been applied in the calculation which follows.

It is necessary to note, however, that one can use a more sophisticated choice for the bulk electrolyte, which then will influence the results for the particle-wall distribution functions. In fact, the EXP 3 choice for the bulk fluid will lead to the EXP 3 (E 3/E 2) form of $g_{xw}(z, \vartheta)$:

$$g_{xw}(z, \vartheta) = g_{xw}^{(EXP2)}(z, \vartheta) \exp\left\{h_{xy}^{(EXP3)} \bigwedge h_{yw}^{(EXP2)} - H_{xy}^{(MSA)} \bigwedge H_{yw}^{(MSA)} - G_{xy}^{(3)} \bigwedge H_{yw}^{(MSA)}\right\} \tag{32}$$

Finally we should like to mention that the RHNC results or even the simulation data can be used as an input for the iterative procedure for the particle-wall distribution functions. The inclusion of the diagrams with two field vertices in (20) can be fulfilled in a similar manner.

The dipole-wall distribution function is expanded according to (15) by the Legendre polynomials. Then the expansion coefficients determine the dipole density profile

$$\varrho_{sw}(z) = \eta(1 - c_i)\, \tilde{g}_{sw}^{(0)}(z), \tag{33}$$

the polarization density profile

$$P^*(z) = \eta(1 - c_i)\, \mu_s^*\, \tilde{g}_{sw}^{(1)}(z) \tag{34}$$

and the normalized angular distribution of dipoles [16]

$$\tilde{g}_{sw}(z, \vartheta) = g_{sw}(z, \vartheta)/2\tilde{g}_{sw}^{(0)}(z). \tag{35}$$

The ion-wall distribution functions provide the density profile of ions and the charge density profile, which both have been already analysed by us in [23, 34].

It is important to note that, unlike the MSA, any of the exponential approximations contains a non-linear dependence on the electric field on the wall E^*. On restriction to EXP 2 one has [23]

$$\tilde{\mu}_s(z) = \varrho^*(z)/\varrho_s\, \tilde{g}_{sw}^{(0)}(z) = \mu_s^*\, \mathcal{L}[G_{sw}(z)], \tag{36}$$

where the argument of the Langevin function $\mathcal{L}(x) = \coth x - 1/x$ is determined by the dipole-wall renormalized potential $G_{sw}(z, \vartheta) = G_{sw}(z)\cos\vartheta$. It is clear that (36) reflects the saturation effect on the electric field E^*. Actually, the dependence expressed by the Langevin function similarly to (36) can be obtained within higher order approximations and particularly EXP 3. To get it, one has to allow for the terms proportional to $\mathcal{P}_0(\cos\vartheta)$ and $\mathcal{P}_1(\cos\vartheta)$ (see (16)) and neglect the harmonics of higher order for each cluster coefficient. This leads simply to the renormalization of the Langevin function argument and provides a much more complicated dependence on the field strength. However, on inclusion of terms proportional to the polynomials $\mathcal{P}_n(\cos\vartheta)$ with $n > 1$ the function $\tilde{\mu}_s(z)$ cannot be expressed in the simple form given by (36).

Let us discuss now the set of results for the particle-wall distribution functions within EXP 3. The dipole density profile in the case of an uncharged wall is shown in Figure 8. Like stated in [15], in the RHNC framework the profile is similar to the hard sphere fluid with the exception of the region near the wall. Contrarily to EXP 2, where $g_{sw}(z) = g_{hs}^{(0)}(z)$, EXP 3 provides lowering of the $\tilde{g}_{hs}^{(0)}(z)$ contact value $\tilde{g}_{sw}^{(0)}(z = \sigma/2) < g_{hs}^{(0)}(\sigma/2)$. The dipole normalized angular distribu-

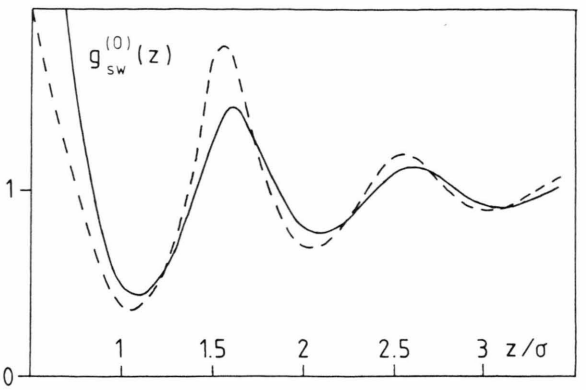

Fig. 8. Dipole density profile $g_{sw}^{(0)}(z)$ near an uncharged hard wall for $E^*=0$, $c_i=10^{-4}$, $q_i^*=119$, $\mu_s^*=2$, $\eta=0.3665$. EXP 2 (full line) results are equal to the Percus-Yevick approximation, EXP 3 (dashed line).

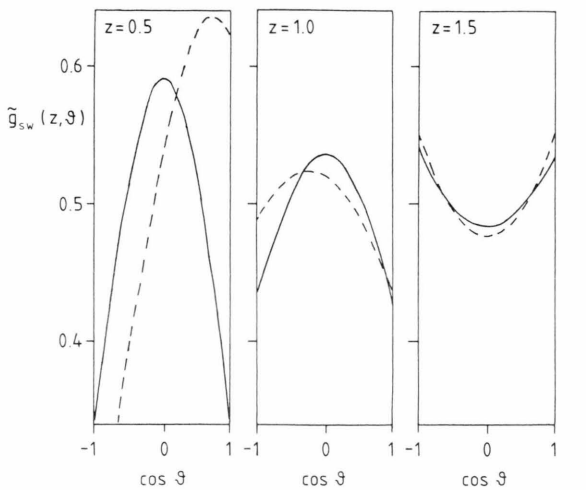

Fig. 9. Normalized orientation density profile $\tilde{g}_{sw}(z, \vartheta)$ for $E^*=0$, $c_i=10^{-4}$, $\mu_s^*=2$ (full line) and for $E^*=1$, $c_i=10^{-1}$, $\mu_s^*=1$ (dashed line). In both cases $q_i^*=119$, $\eta=0.3665$.

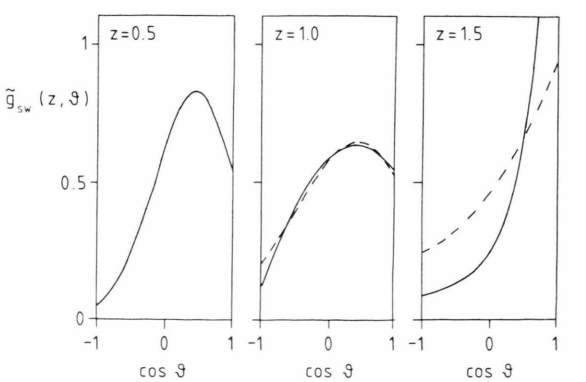

Fig. 10. Normalized orientation density profile for $E^*=2$, $c_i=10^{-2}$, $q_i^*=168$, $\mu_s^*=3.59$, $\eta=0.4012$, EXP 3 (full line), linearized third cluster coefficient approximation [24] (dashed line).

tion at several distances from the wall is shown in the Figure 9. The conclusions which one can get from the EXP 3 data coincide with the RHNC picture [15]. The dipoles prefer to align parallel to the wall near contact and the orientational ordering diminishes at larger distances. In the region of the second peak in the density the dipoles prefer to orientate in the normal direction. The $\cos\vartheta$ distribution is symmetrical at $E^*=0$. In the presence of an electric field the dipoles tend to orientate along the field direction. This effect is much more pronounced in the contact plane then at larger distances where the field is essentially screened by the ions present. With increasing field (Fig. 10), in spite of the presence of ions the solvent becomes polarized even at larger distances from the wall. The angular distribution of dipoles in this case is very similar to the one for the pure dipole fluid near a charged wall [17]. In fact this distribution is in general also very similar to the one obtained by means of MD simulation for the BJH model of water near a Pt wall [35]. It is possible for us to present the $\cos\vartheta$ distribution for the solvent layers as in [9, 35]. This will actually provide smoother curves but will not change their shape.

We have presented the polarization density profiles and the corresponding $\cos\vartheta$ distribution for the ion-dipole mixture at high temperatures and comparatively weak fields (Figures 11, 12) at different ionic concentrations. One has to conclude that qualitative changes in the local structure occur with increasing concentration of the ions. At lower concentration both exponentials lead to the MSA-like polarization profile [36] while at high c_i the $P(z)$ curve is oscillatory around the abscissa. A similar result has been obtained and discussed in [37] within the RHNC theory and by means of simulation in [9].

In order to illustrate the crucial importance to allow for the cluster coefficients efficiently at the application of the OCE we present the screening potential of the dipole-wall interaction and the expansion coefficients of the third cluster term $G_{sw}^{(3)}(z, \vartheta)$ in the Figure 13. With increasing order n of the expansion coefficient, $G_{sw}^{(3)n}(z)$ decreases. However $G_{sw}^{(3)0}(z)$ influences strongly the density effects and the influence of $G_{sw}^{(3)10}(z)$ can be more essential than the one due to the screening effect. It is evident how careful one has to be with the truncation of the OCE and with the interpretation of the results. Anyway, one can conclude in general that the EXP 3 form is appropriate for the qualitative description of the solvents local struc-

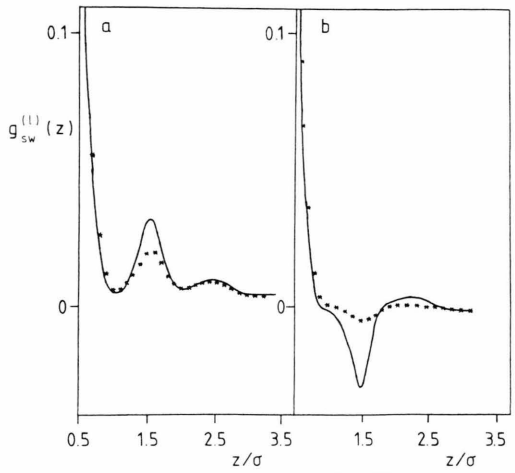

Fig. 11. Polarization density profile $g_{sw}^{(1)}(z)$. Dependence on the ion concentration: $c_i = 10^{-2}$ (a), $c_i = 0.5$ (b). $E^* = 0.25$, $q_i^* = 16$, $\mu_s^* = 3.59$, $\eta = 0.4$. EXP 3 (full line), EXP 2 (***).

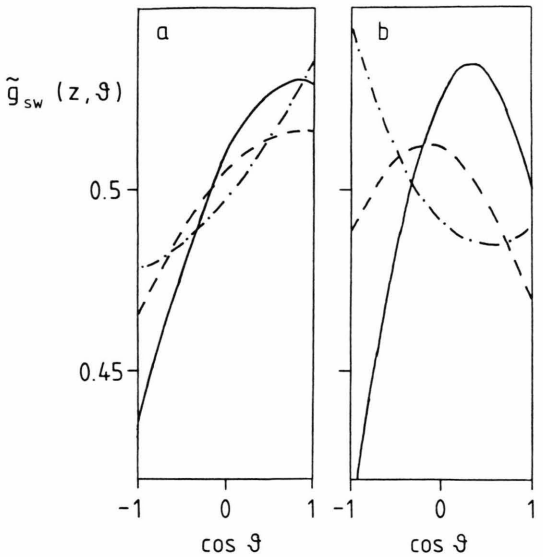

Fig. 12. Normalized orientation density profile. The parmeters are as in Fig. 11, $z/\sigma = 0.5$ (full line), $z/\sigma = 1.0$ (dashed line), $z/\sigma = 1.5$ (dash dot curve).

ture for electrolyte solutions near a charged or uncharged hard wall.

We should like to discuss now one more point which is helpful and necessary in order to provide the comparison of theoretical and simulation results. Usually, while simulating aqueous systems in a contact with a crystal surface one utilizes the coverage parameter ϑ_s (see, for instance [10]). It can be treated as an input parameter for a given simulation and is

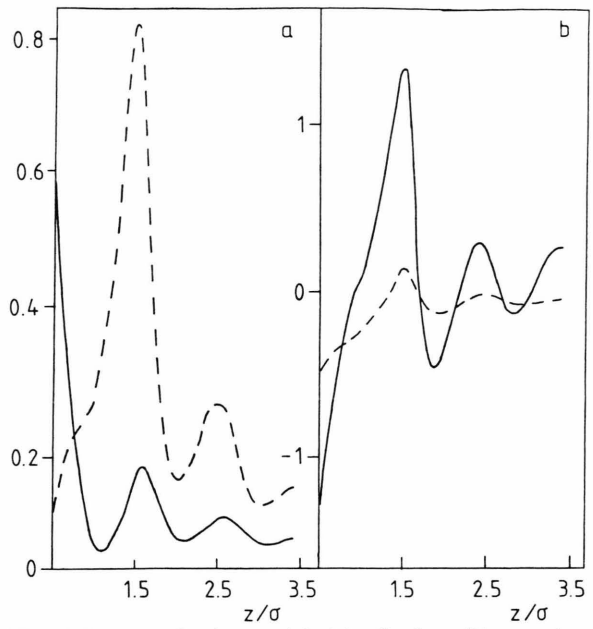

Fig. 13. Renormalized potential of the dipole-wall interaction $G_{sw}(z)$ and the expansion coefficients of the third cluster term. a: $G_{sw}(z)$ (full line), $G_{sw}^{(3)10}(z)$ (dashed line). b: $G_{sw}^{(3)00}(z)$ (full line), $G_{sw}^{(3)20}(z)$ (dashed line). $E^* = 2.0$, $c_i = 10^{-2}$, $q_i^* = 168$, $\mu_s^* = 3.59$, $\eta = 0.4$

determined as the number ratio of absorbed water molecules on the crystal sites and the total number of sites per unit area. We should like to show that it is possible to define and deal with the coverage parameter in the theory. The method then looks in a simplified form as follows.

If the short-range interaction between the dipole particle i and the site α in the crystal plane is assumed to be of Lennard-Jones type,

$$U_{ws}(i, \alpha) = 4e[(\sigma_{ws}/r_{i\alpha})^{12} - (\sigma_{ws}/r_{i\alpha})^{6}], \tag{37}$$

then the dipole particle i can be considered in an external potential formed by the crystal sites

$$U_{ws}(u) = \sum_{\alpha} U_{ws}(i, \alpha), \tag{38}$$

where the sum is taken over the sites on the surface plane. The singlet theories [38, 39] developed to date deal usually with potentials which depend only on z. Therefore the potential (38) can be replaced by an effective one-dimensional interaction [40] for instance of the type

$$U_{ws}(z) = 2\pi n \varepsilon \sigma_{ws}^2 [\tfrac{2}{5}(\sigma_{ws}/z)^{10} - (\sigma_{ws}/z)^4]. \tag{39}$$

This means that the crystal structure of the last plane of the solid is replaced by a continuous distribution of

Lennard-Jones atoms with the same planar density $n = N_{\text{sites}}/S$. The model with the soft-core wall interaction can be transformed into the model with a hard wall by the blip function method. The latter is then decribed by the two-dimensional packing fraction parameter $\eta_l = n l^2/4$, where l is the lattice vector. One can determine the total number of solvent particles in the first monolayer from the definition of the profile

$$N_T = \tfrac{1}{2} \varrho_s \int g_{sw}(x, y, z, \vartheta)\, dx\, dy\, dz \sin\vartheta\, d\vartheta$$

$$= \frac{3\eta}{\pi\sigma_s^2} S \int_0^{\pi} \sin\vartheta\, d\vartheta \int_0^{1/2} g_{sw}(z, \vartheta)\, dz, \qquad (40)$$

where S is the surface area. Then the absorbent packing fraction γ is

$$\gamma = \frac{\pi N_T \sigma_s^2}{4S} = \tfrac{3}{4}\eta \int_0^{\pi} \sin\vartheta\, d\vartheta \int_0^{1/2} g_{sw}(z, \vartheta)\, dz. \qquad (41)$$

Now the coverage parameter can be defined as the ratio of two packing fractions

$$\vartheta_s = \gamma/\eta_l = \tfrac{3}{4}(\eta/\eta_l) \int_0^{\pi} \sin\vartheta\, d\vartheta \int_0^{1/2} g_{sw}(z, \vartheta)\, dz. \qquad (42)$$

This relation can be used when comparing theoretical results with simulation data.

Acknowledgement

It is a pleasure to thank P. Bopp, M. F. Holovko, and E. Spohr for many helpful discussions. O. A. Pizio thanks A. D. J. Haymet and his co-workers for their hospitality during his stay at University of Utah in Salt Lake City.

[1] K. Heinzinger, Physica **131 B,** 196 (1985).
[2] K. Heinzinger and G. Palinkas, in: The Chemical Physics of Solvation, part A (R. R. Dogonadze et al., eds.), Elsevier, Amsterdam 1985.
[3] K. Heinzinger, in: Computer Modelling of Fluids, Polymers and Solids (C. R. A. Catlow et al., eds.), Kluwer Academic Publ., 1990.
[4] P. Bopp, G. Jancso, and K. Heinzinger, Chem. Phys. Lett. **98,** 129 (1983).
[5] G. Jancso, P. Bopp, and K. Heinzinger, Chem. Phys. **85,** 377 (1984).
[6] P. Bopp, I. Okada, H. Ohtaki, and K. Heinzinger, Z. Naturforsch. **40 a,** 116 (1985).
[7] E. Spohr and K. Heinzinger, J. Chem. Phys. **79,** 3467 (1986).
[8] E. Spohr and K. Heinzinger, Chem. Phys. Lett. **123,** 218 (1986).
[9] E. Spohr, J. Phys. Chem. **93,** 6171 (1989).
[10] E. Spohr and K. Heinzinger, Electrochim. Acta **33,** 1211 (1988).
[11] J. M. Caillol, D. Levesque, and J. J., Weis, Mol. Phys. **69,** 199 (1990).
[12] P. G. Kusalik and G. N. Patey, J. Chem. Phys. **88,** 7715 (1988).
[13] P. G. Kusalik and G. N. Patey, J. Chem. Phys. **89,** 5843 (1988).
[14] P. G. Kusalik and G. N. Patey, J. Chem. Phys. **89,** 7478 (1988).
[15] W. Dong, M. L. Rosinberg, A. Perera, and G. N. Patey, J. Chem. Phys. **89,** 4994 (1988).
[16] V. Russier, M. L. Rosinberg, J. P. Badiali, D. Levesque, and J. J. Weis, J. Chem. Phys. **87,** 5012 (1987).
[17] V. Russier, J. Chem. Phys. **90,** 4491 (1989).
[18] P. J. Rossky, Rev. Phys. Chem. **36,** 321 (1985).
[19] T. Ichiye and A. D. J. Haymet, J. Chem. Phys. **89,** 4315 (1988).
[20] M. F. Holovko, O. A. Pizio, and A. D. Trokhymchuk, Preprint Inst. for Theor. Phys. No. 87-155 E, Kyjiv 1987 (submitted to Z. Naturforsch.).
[21] A. D. Trokhymchuk and O. A. Pizio, submitted to Z. Naturforsch.
[22] O. A. Pizio, M. F. Holovko, and A. D. Trokhymchuk, Acta Chim. Hung. **125,** 385 (1988).
[23] M. F. Holovko, S. N. Blotskyj, and O. A. Pizio, Electrochim. Acta **34,** 63 (1989).
[24] S. N. Blotskyj, M. F. Holovko, O. A. Pizio, and E. Spohr, Preprint Inst. for Theor. Phys. No. 89-20 E, Kyjiv 1989.
[25] M. F. Holovko, I. I. Kurilijak, O. A. Pizio, and E. N. Sovijak, in: Problems fo Contemporary Statistical Physics (N. N. Bogoljubov, ed.), Naukova Dumka, Kyjiv 1985.
[26] M. F. Holovko and I. R. Yukhnovskij, in: The Chemical Physics of Solvation, part A (R. R. Dogonadze et al., eds.), Elsevier, Amsterdam 1985.
[27] L. Blum and F. Vericat, in: The Chemical Physics of Solvation, part A (R. R. Dogonadze et al., eds.), Elsevier, Amsterdam 1985.
[28] P. Linse and H. C. Andersen, J. Chem. Phys. **85,** 3027 (1986).
[29] K. Y. Chan, K. E. Gubbins, D. Henderson, and L. Blum, Mol. Phys. **66,** 299 (1989).
[30] I. R. Yukhnovskij and M. F. Holovko, Statistical Theory of Classic Equilibrium Systems, Naukova Dumka, Kyjiv 1980.
[31] D. Henderson, F. F. Abraham, and J. A. Barker, Mol. Phys. **31,** 1291 (1976).
[32] J. K. Percus, J. Stat. Phys. **15,** 1772 (1976).
[33] L. Blum and D., Henderson, J. Chem. Phys. **74,** 1902 (1981).
[34] M. F. Holovko, S. N. Blotskyj, and O. A. Pizio, Ukrainian Phys. J. **35,** 585 (1990).
[35] G. Nagy, E. Spohr, and K. Heinzinger, private communication.
[36] F. Vericat, L. Blum, and D. Henderson, J. Chem. Phys. **77,** 5808 (1982).
[37] G. M. Torrie, P. G. Kusalik, and G. N. Patey, J. Chem. Phys. **90,** 4513 (1989).
[38] M. Plischke and D. Henderson, J. Chem. Phys. **88,** 2712 (1988).
[39] M. Plischke and D. Henderson, J. Chem. Phys. **84,** 2846 (1986).
[40] J. P. Badiali, M. E. Boud-Hir, and V. Russier, J. Electroanal. Chem. **184,** 41 (1985).